A&A 480, 581–587 (2008)
DOI: 10.1051/0004-6361:20078437

Astronomy & Astrophysics

Self-broadening of the hydrogen Balmer α line

N. F. Allard[1,2], J. F. Kielkopf[3], R. Cayrel[4], and C. van 't Veer-Menneret[4]

[1] Institut d'Astrophysique de Paris, UMR 7095, CNRS, Université Pierre et Marie Curie, 98bis boulevard Arago, 75014 Paris, France
e-mail: allard@iap.fr
[2] Observatoire de Paris-Meudon, LERMA, UMR 8112, CNRS, 92195 Meudon Principal Cedex, France
[3] Department of Physics and Astronomy, University of Louisville, Louisville, KY, 40292, USA
[4] Observatoire de Paris-Meudon, GEPI, UMR 8111, CNRS, 92195 Meudon Principal Cedex, France

Received 7 August 2007 / Accepted 14 December 2007

ABSTRACT

Context. Profiles of hydrogen lines in stellar spectra are determined by the properties of the hydrogen atom and the structure of the star's atmosphere. Hydrogen line profiles are therefore a very important diagnostic tool in stellar modeling. In particular they are widely used as effective temperature criterion for stellar atmospheres in the range $T_{\rm eff}$ 5500–7000 K.
Aims. In cool stars such as the Sun hydrogen is largely neutral and the electron density is low. The line center width at half maximum and the spectral energy distribution in the wings are determined primarily by collisions with hydrogen atoms due to their high relative density. This work aims to provide benchmark calculations of Balmer α based on recent H_2 potentials.
Methods. For the first time an accurate determination of the broadening of Balmer α by atomic hydrogen is made in a unified theory of collisional line profiles using ab initio calculations of molecular hydrogen potential energies and transition matrix elements among singlet and triplet electronic states.
Results. We computed the shape, width and shift of the Balmer α line perturbed by neutral hydrogen and studied their dependence on temperature. We present results over the full range of temperatures from 3000 to 12 000 K needed for stellar spectra models.
Conclusions. Our calculations lead to larger values than those obtained with the commonly used Ali & Griem (1966, Phys. Rev. A, 144, 366) theory and are closer to the recent calculations of Barklem et al. (2000a, A&A, 355, L5; 2000b, A&A, 363, 1091). We conclude that the line parameters are dependent on the sum of many contributing molecular transitions, each with a different temperature dependence, and we provide tables for Balmer α. The unified line shape theory with complete molecular potentials also predicts additional opacity in the far non-Lorentzian wing.

Key words. line: profiles – stars: atmospheres – stars: white dwarfs

1. Introduction

The optical spectra of stars exhibit the Balmer lines of hydrogen perturbed by neutral hydrogen, electrons, protons, and smaller concentrations of other neutral and ionized atoms. When the surface effective temperature is low the collisional effects are mainly due to neutral perturbers. Consider, for example, a Kurucz (1993) model atmosphere, for $T_{\rm eff}$ = 5777 K , log g = 4.44, and a metalicity 1/100th of solar with an enhancement in α-elements of 0.4 dex (a metal-poor Sun). Under these conditions, a ratio of densities of neutral hydrogen atoms to electrons $n_{\rm H}/n_{\rm e} \approx 8000$, at a Rosseland optical depth of unity, and the contribution of the self-resonance broadening at 5 Å from the line center of Balmer α is three times larger than that of the Stark effect. While this ratio decreases with increasing temperature, it remains larger than that of turn-off stars. Consequently, a reliable broadening by neutral hydrogen collisions is a "must" for stellar diagnostics.

Ali & Griem (1966) calculated the resonance broadening based on a multipole expansion of the interaction, neglecting so-called van der Waals interactions. Their work was widely adopted for use in stellar atmosphere models. Recently, Barklem et al. (2000a) presented a theory of self-broadening of hydrogen lines which included long range resonance and van der Waals effects, especially accurate for the critical long-range interactions responsible for line broadening. When applied to cool stars the new work resulted in significantly different line profiles compared with previous theories (Barklem et al. 2000b). Nevertheless, discrepancies were noted between these models and solar and stellar spectra observed at high resolution.

Broadening of the core of Balmer series lines of hydrogen by neutral hydrogen collisions has never been measured in the laboratory. Since the underpinning atomic physics is understood, theoretical models may be progressively improved by including more complete representations of the interaction, especially in the region of atom separations which determine the line width. Furthermore, the change of radiative transition moment with atomic separation has a significant effect on the line wings and also can alter the width. These effects have heretofore not been included in Balmer line widths used in astrophysical applications. Our results also show a significant dependence of the broadening on relative atomic velocity, and as a consequence demonstrate that an explicit calculation of the line width averaging over the thermal velocity distribution is needed. Tables for the contributions to the width from representative contributing molecular states, and sums for the 3d–2p, 3p–2s, and 3s–2p components, show that properly averaging over velocity, increases the width compared to using a mean velocity representative of the temperature.

For our purposes it is fortunate that H_2 is very well studied. Precise asymptotic energies and transition dipole moments are known, and remarkable recent improvements in computational accuracy and speed allow their determination at all atomic separations for the lower electronic states of H_2 that are needed to understand the Balmer α atomic line. Here we use the recent

ab initio calculations made by Spielfiedel (2003, 2004, and references therein). These potentials give the interaction for all values of R. They have the correct asymptotes, and their limitations in accuracy at long range have been studied.

Parallel progress in unified line broadening theory now enables us to calculate neutral atom spectra given the energies and radiative transition moments for relevant states of the radiating atom interacting with other atoms in its environment. In a unified treatment, the complete spectral energy distribution is computed from the core to the far line wing. The Lorentzian width and shift can be readily extracted, and the far wing quantitatively examined, for all of the components that may contribute to a line, even one as complex as Balmer α. Details of the fundamental theory are presented in Allard & Kielkopf (1982) and in Allard et al. (1999).

In the upper atmosphere of the cool stars under consideration, the neutral hydrogen atom density is of the order of 10^{15} cm^{-3} in the region of line core formation (Kurucz 1979; Cox 1999). Under these low density conditions we expect that the impact approximation will be a good starting point for synthetic spectra, with the understanding that it will not give a correct line wing. In impact broadening, the duration of the collision is assumed to be small compared to the interval between collisions, and the results describe the line within a few line widths of center. The impact theories of pressure broadening (Baranger 1958a,b; Kolb & Griem 1958) are based on the assumption of sudden collisions (impacts) between the radiator and perturbing atoms, and are valid when frequency displacements $\Delta\omega = \omega - \omega_0$ and gas densities are sufficiently small. One outcome of our unified approach is that we may evaluate the difference between the impact limit and the general unified profile, and establish with certainty the region of validity of an assumed Lorentzian profile.

In Sect. 2.1 which follows, we review briefly the unified theory we use to evaluate the line shape in the context of the present study, and the limitations set by the potentials and transition moments. In Sect. 3, we summarize the results obtained for temperatures 3000 to 12 000 K, and compare widths with our methods to the values obtained in the Ali & Griem (1966) theory, and the work of Barklem et al. (2000a,b).

2. General expression for the spectrum

2.1. Unified theory

Our theoretical approach is based on the quantum theory of spectral line shapes of Baranger (1958a,b) developed in an *adiabatic representation* to include the degeneracy of atomic levels (Royer 1974, 1980; Allard et al. 1994).

Although our unified theory has been developed in Allard et al. (1999), and a detailed discussion is presented there, we review here the main results. The fundamental expression of the normalized spectrum is given by

$$I(\Delta\omega) = \frac{1}{\pi}\,\mathrm{Re}\int_0^{+\infty}\Phi(s)\mathrm{e}^{-\mathrm{i}\Delta\omega s}\mathrm{d}s. \tag{1}$$

The dipole autocorrelation function for a perturber density n_p is

$$\Phi(s) = \mathrm{e}^{-n_\mathrm{p} g(s)}, \tag{2}$$

where decay of the autocorrelation function with time leads to atomic line broadening.

For a transition $\alpha = (i, f)$ from an initial state i to a final state f, we have

$$g_\alpha(s) = \frac{1}{\sum_{e,e'}^{(\alpha)}|d_{ee'}|^2}\sum_{e,e'}^{(\alpha)}\int_0^{+\infty}2\pi\rho\mathrm{d}\rho\int_{-\infty}^{+\infty}\mathrm{d}x\,\tilde{d}_{ee'}[\,R(0)\,] \times\left[\mathrm{e}^{\frac{\mathrm{i}}{\hbar}\int_0^s \mathrm{d}t\,V_{e'e}[\,R(t)\,]}\,\tilde{d}^*_{ee'}[\,R(s)\,] - \tilde{d}_{ee'}[\,R(0)\,]\right]. \tag{3}$$

This expression depends on an adiabatic approximation at the one-perturber level, in which we neglect the effect of transitions induced between different electronic states. As explained in the theoretical development by Allard et al. (1999), the neglect of this effect is not expected to be significant for neutral collisions such as we consider here. Barklem et al. (2000b) also discuss this point, and suggest that because the duration of the collision is so short compared to the time scale for internal atomic processes, ℓ-changing collisions will not affect the line width. We do, however, allow for variation of the transition moment during the collision which takes into account the mixing of atomic states resulting from the pseudo-static interaction with the perturbing atom.

The e and e' label the energy surfaces on which the interacting atoms approach the initial and final atomic states of the transition as $R \to \infty$. The asymptotic initial and final state energies are E_i^∞ and E_f^∞, such that $E_e(R) \to E_\mathrm{i}^\infty$ as $R \to \infty$. We then have R-dependent frequencies

$$\nu_{e'e}(R) \equiv (E'_e(R) - E_e(R))/h\,, \qquad e \in \varepsilon_\mathrm{i},\ e' \in \varepsilon_\mathrm{f} \tag{4}$$

which become the isolated radiator frequency ν_if when perturbers are far from the radiator.

For the $n_\mathrm{i} = 2$, and $n_\mathrm{f} = 3$ levels there are many energy surfaces which lead to the same asymptotic energy at $R \to \infty$, between which, finally, there are 36 allowed molecular transitions which contribute to Balmer α.

The total line strength of the transition is $\sum_{e,e'}|d_{ee'}|^2$. The radiative dipole transition moment of each component of the line depends on R, and changes during the collision. At time t from the point of closest approach for a rectilinear classical path

$$R(t) = \left[\rho^2 + (x + vt)^2\right]^{1/2}, \tag{5}$$

where ρ is the impact parameter of the perturber trajectory, and x is the position of the perturber along its trajectory.

In the present context, the perturbation of the frequency of the atomic transition during the collision results in a phase shift, $\eta(s)$, calculated along a classical path $R(t)$ that is assumed to be rectilinear. The phase shift is

$$\eta(s) = \frac{i}{\hbar}\int_0^s \mathrm{d}t\;V_{e'e}[\,R(t)\,] \tag{6}$$

where $\Delta V(R)$, the difference potential, is given by

$$\Delta V(R) \equiv V_{e'e}[R(t)] = V_{e'}[R(t)] - V_e[R(t)], \tag{7}$$

and represents the difference between the electronic energies of the quasi-molecular transition.

An atomic line broadened by collisions in a low density gas has a Lorentzian profile near the line center which can be related to the Fourier Transform of a radiative wave in which short duration collisions produce sudden phase changes. In the theory of impact broadened line shapes the phase shifts are given by Eq. (6) with the integral taken between $s = 0$ and ∞. At sufficiently low densities of the perturbers the symmetric center of a

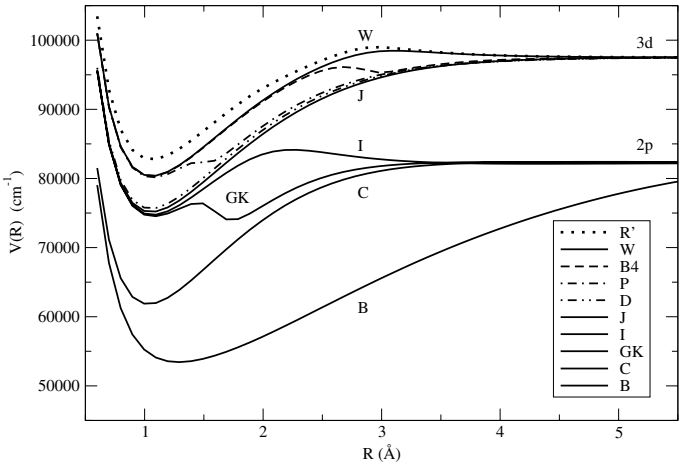

Fig. 1. Molecular potentials for H_2 correlated to the 3d and 2p singlet states of atomic H. The energies from Spielfiedel et al. (2004) are given relative to the asymptotic atomic state. See Table 4 for transition identifications.

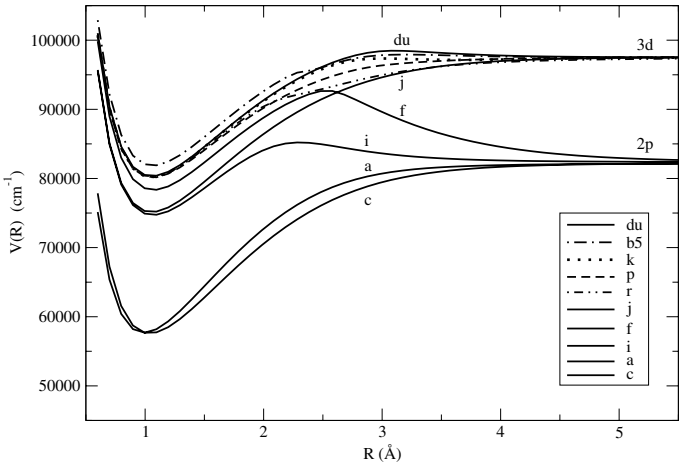

Fig. 2. Molecular potentials for H_2 correlated to the 3d and 2p triplet states of atomic H. The energies from Spielfiedel et al. (2004) are given relative to the asymptotic atomic state. See Table 4 for transition identifications.

spectral line is Lorentzian and can be defined by two line parameters, the width and the shift of the main line. These quantities can be obtained in the impact limit ($s \to \infty$) of the general calculation of the autocorrelation function (Eq. (3)). In the following discussion we refer to this line width as measured by half the full width at half the maximum intensity, what is customarily termed HWHM.

2.2. Molecular potentials and dipole moments

The potentials and radiative dipole transition moments are input data for a unified spectral line shape evaluation. For the complete Balmer α resonance line profile we have plotted in Figs. 1 and 2 the potential energies correlated to the 3d and 2p states as computed by Spielfiedel et al. (2004). The 20 transitions which generate the 3d–2p component provide the main contribution to Hα line broadening. See Table 4 in the Appendix for transition identifications. In the table for each transition we give the asymptotic d^2 in atomic units, the square of the radiative electric dipole transition moment of the atomic transition.

3. Results

Previous calculations by Barklem et al. (2000a,b) predict a line width which increases with temperature in contradiction to the Ali & Griem (1966) theory. They explain this different behavior in their calculations by the increasing departure at decreasing R from the purely R^{-3} dependence of the interaction on the interatomic separation which was the basis of the Ali & Griem (1966) work. An important feature of their new theory is that the dispersive-inductive components of the interaction (van der Waals force) have been included accurately. Our calculations do this as well, and we include addtionally the dependence of the radiative dipole transition moment on interatomic separation. To this end, we employ the complete set of molecular potentials for the states contributing to the transition. These potentials are precisely accurate at small and intermediate R, verified by consistent agreement with other a priori evaluations, and with experimentally determined stable states of H_2. Spielfiedel et al. (2004) also have shown that while the potentials may have lower precision at long range, they exhibit the correct asymptotic behavior.

To verify if the long range interaction is solely the most important region of the potential determining the line width in broadening due to collisions between two neutral atoms, Allard & Biraud (1983) studied the effect of the different regions of the interaction on the line profile using a two-step potential. They demonstrated that the width is given mainly by the strong interaction typically when atoms are close, rather than the very long range part. This was the fundamental physical idea of Weisskopf (1933) who considered that the broadening arises essentially from collisions which cause phase changes η greater than 1. Their result confirmed studies by Roueff & Regemorter (1969) and by Lortet & Roueff (1969) of collisions with light atoms whose polarizability is small. It was shown by them that the width of spectral lines due to collisions with hydrogen atoms arises not only from the Van der Waals dispersion forces but significantly from interactions at an even shorter range. On the other hand, since the shift is mainly due to a weak interaction of distant perturbers, the description of the line core requires knowledge of the long range asymptotic potential. These results have been pointed out before by Sahal-Bréchot (1969) and Roueff & Regemorter (1969). The immediate consequence for this case is that we expect the resonance broadening of atomic hydrogen will depend on the interactions of colliding atoms not only at large R, but at intermediate and small R as well.

To show how different this variation is among the individual transitions, we selected 6 transitions contributing to Balmer α which have the largest line widths and show the results for individual triplet transitions in Table 1 and Fig. 3. The line parameters depend on $\Delta V(R)$, the difference between the ground and excited state interaction potentials. Figure 4 shows the general behavior over all R. A more detailed view at intermediate R is shown for a few states in Figs. 5 and 6. The complexity of the small change in the potential difference as the atoms approach from a long range asymptotic behavior into the strong interactions usually associated with bound states and chemical reactions produces phase shifts in unbound transient collisions, and contributes to the line width. These contributions cannot be adequately evaluated without knowledge of the details of the behavior at intermediate R. It is this behavior that requires use of complete potentials in the line shape calculation in order to be confident that the line width is accurately determined.

Table 1. Variation of the half-width at half maximum intensity (HWHM) (10^{-8} rad s^{-1} cm^3) with temperature computed with $\bar{v}$ for the 6 strongest triplet transitions of the 3d–2p component.

HWHM	Upper Level	Lower Level	5000	6000	7000	8000	9000	10 000	11 000	12 000	d^2
r–f	2–$^3\Pi_g$	3–$^3\Sigma_u^+$	0.391	0.401	0.408	0.415	0.422	0.429	0.435	0.439	4.5
du–i	1–$^3\Delta_u$	1–$^3\Pi_g$	0.377	0.364	0.350	0.343	0.332	0.329	0.321	0.314	9
k–a	3–$^3\Pi_u$	1–$^3\Sigma_g^+$	0.289	0.279	0.271	0.264	0.258	0.252	0.248	0.244	4.5
j–c	1–$^3\Delta_g$	1–$^3\Pi_u$	0.276	0.264	0.252	0.242	0.233	0.225	0.218	0.213	9
p–f	4–$^3\Sigma_g^+$	3–$^3\Sigma_u^+$	0.26	0.261	0.263	0.265	0.266	0.267	0.269	0.270	6
b5–a	5–$^3\Sigma_u^+$	1–$^3\Sigma_g^+$	0.245	0.246	0.245	0.244	0.242	0.241	0.241	0.241	6.

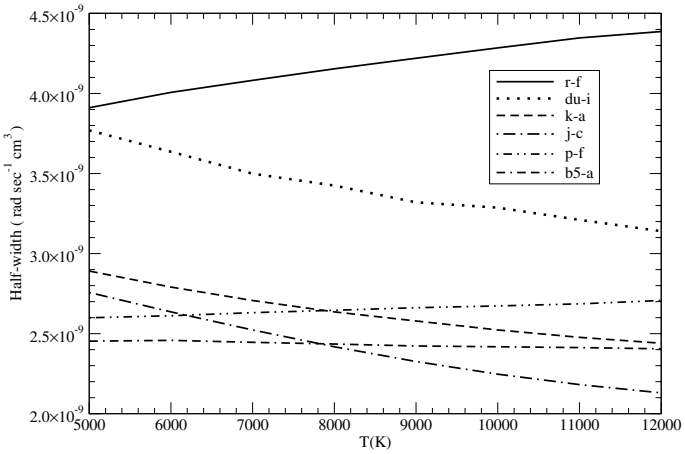

Fig. 3. Variation of the line width (HWHM) per perturber with temperature for the 6 strongest transitions of the 3d–2p component.

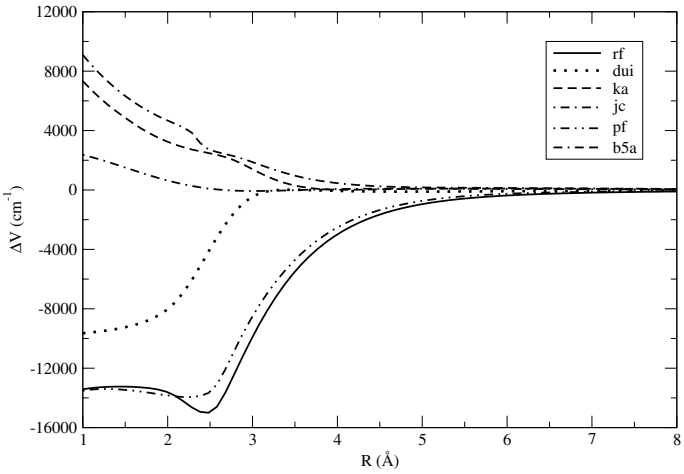

Fig. 4. Potential difference for the 6 strongest transitions of the 3d–2p component.

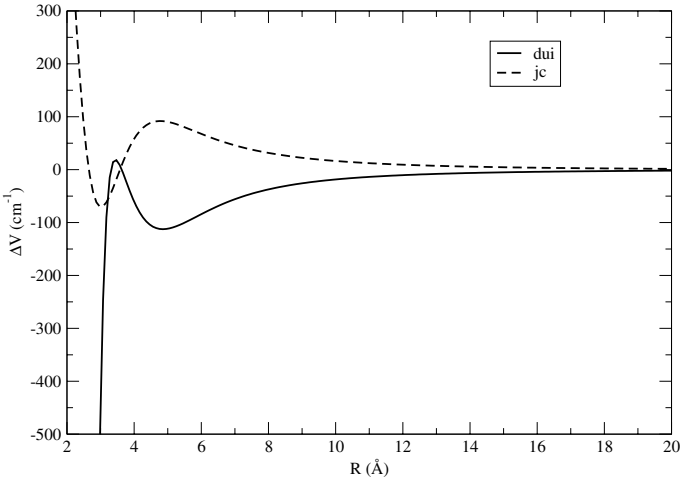

Fig. 5. Potential difference for the j–c and du–i triplet transitions contributing to Balmer α.

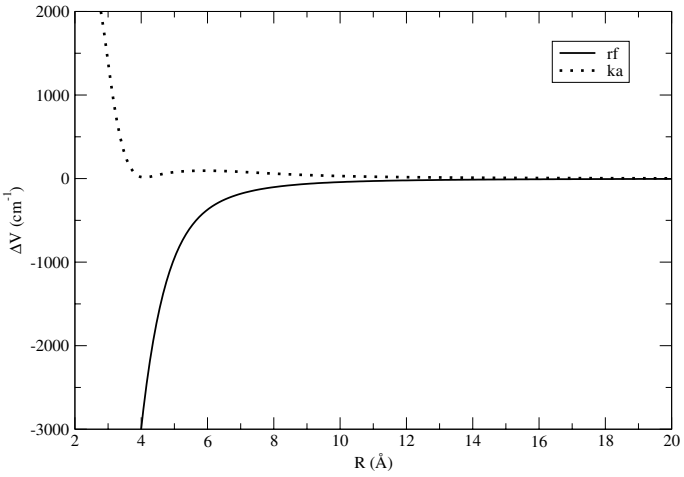

Fig. 6. Potential difference for the k–a and r–f triplet transitions contributing to Balmer α.

To study the influence of temperature we investigated the effect of averaging over velocity in the theoretical evaluation. It has been common practice to use a single fixed mean velocity $\bar{v}$ in the calculation of impact broadening, as was done by Ali & Griem (1966). Barklem et al. (2000a,b) fit the dependence of the cross section on v to a power law and average analytically. In our work this averaging was done numerically by performing the calculation for different velocities and then thermally averaging with 24-point Gauss-Laguerre integration. Table 2 reports the line widths determined with averaging over the velocity, and with using an average velocity, for the entire profile, and also details the contributions from the different 3d–2p, 3p–2s and 3s–2p components of Balmer α.

Figures 7 and 8 show respectively the variation of the line width and the line shift with temperature for the different components 3d–2p, 3p–2s and 3s–2p contributing to Balmer α. There is a slight non-linear 11% increase in width with temperature from 3000 K to 12 000 K evident in the calculations done by averaging over velocity. Averaging over velocities also increased the width by about 15% compared to using a mean velocity for the

Table 2. Variation of the half-width at half maximum intensity (HWHM) per perturber (10^{-8} rad s^{-1} cm^3) with temperature. Total Hα and contributions of the 3d2p, 3p2s, 3s2p components.

HWHM		3000	4000	5000	6000	7000	8000	9000	10 000	11 000	12 000
Total H α	$\bar{v}$	3.45	3.47	3.51	3.53	3.54	3.57	3.61	3.65	3.67	3.67
	aver	4.03	4.14	4.21	4.26	4.3	4.35	4.4	4.43	4.45	4.49
3d–2p	$\bar{v}$	2.95	2.91	2.89	2.87	2.85	2.85	2.84	2.84	2.83	2.82
	aver	3.51	3.55	3.58	3.58	3.59	3.60	3.60	3.61	3.61	3.62
3p–2s	$\bar{v}$	0.41	0.45	0.51	0.55	0.57	0.61	0.65	0.68	0.71	0.72
	aver	0.43	0.48	0.52	0.56	0.59	0.63	0.66	0.69	0.71	0.73
3s–2p	$\bar{v}$	0.09	0.09	0.10	0.11	0.11	0.12	0.12	0.13	0.13	0.13
	aver	0.1	0.1	0.11	0.12	0.12	0.13	0.13	0.14	0.14	0.15

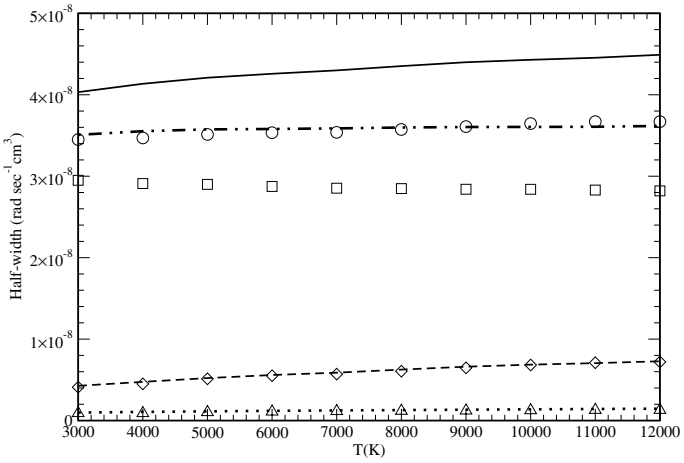

Fig. 7. Comparison of the line width of the contributions of the different components, 3d–2p, 3p–2s and 3s–2p, due to H-H collisions with temperature in the different approaches using a single velocity $\bar{v}$ and averaging over velocity. (—) Total of all contributions averaged over velocity; (∘ ∘ ∘) total using $\bar{v}$; (– · · – · · –) 3d–2p only, averaged over velocity; (□) 3d–2p only, using $\bar{v}$; (– – –) 3p–2s only, averaged over velocity; (◇) 3p–2s only, using $\bar{v}$; (· · ·) 3s–2p only, averaged over velocity; (△) 3s–2p only, using $\bar{v}$.

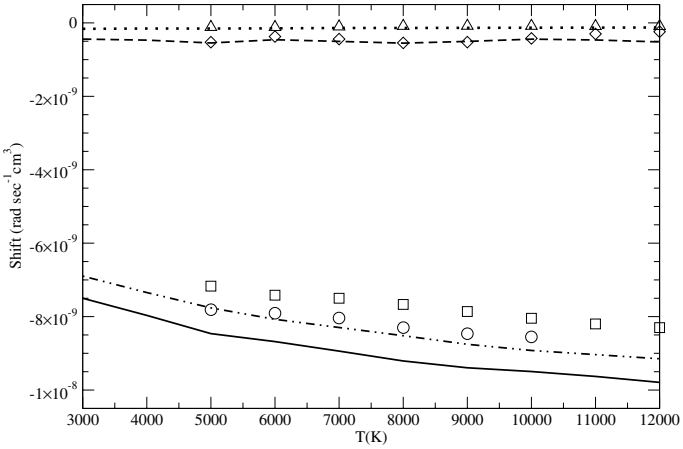

Fig. 8. Comparison of the line shift of the contributions of the different components, 3d–2p, 3p–2s and 3s–2p, due to H-H collisions with temperature in the different approaches using a single velocity $\bar{v}$ and averaging over velocity. Same symbols as in Fig. 7. (—) Total of all contributions averaged over velocity; (∘ ∘ ∘) total using $\bar{v}$; (– · · – · · –) 3d–2p only, averaged over velocity; (□) 3d–2p only, using $\bar{v}$; (– – –) 3p–2s only, averaged over velocity; (◇) 3p–2s only, using $\bar{v}$; (· · ·) 3s–2p only, averaged over velocity; (△) 3s–2p only, using $\bar{v}$.

calculations. Also, the results from a mean velocity are nearly independent of temperature because the contribution from the 3d–2p transition decreases with temperature. When averaging over velocity, there is a very slight increase with temperature for this component. We conclude that because of these subtle effects, averaging velocity is quite important to obtain an accurate Balmer α line core. In Fig. 9 we have plotted the contributions of the singlets and of the triplets to the 3d–2p component. The significance of averaging over velocity is apparent in each contributing transition.

Our calculations are compared with those of Ali et al. in Fig. 10, and in Table 3, where the values of Barklem shown were extracted from Fig. 3 of Barklem et al. (2000b). Our calculations agree with the results of Barklem et al. (2000a,b) that the commonly used Ali & Griem theory very significantly underestimates the line width of Balmer α. The data shown in the figure also illustrate the necessity of including the entire complex structure of Balmer α to obtain at the correct width that is useful in stellar models.

In Fig. 11 we compare our calculation of the complete unified theory line profile using Eq. (3) to the Lorentzian profile using the impact limit. As noted by Barklem et al. (2000b), the impact approximation is not valid outside 7 Å from the center for the density of $n_{\rm H} = 1 \times 10^{18}$ cm^{-3} used in this example. The unified theory profile includes the contributions of radiative transitions during collision, sometimes termed *quasi-molecular* spectra. These events add to the wing of the line, and are an additional source of opacity for stellar atmospheres (Allard et al. 2004). The Lorentzian profile shown in the figure is a useful representation of the unified line shape from 6540 to 6580 Å.

It is interesting to check the influence of the moderate change of our results with respect to those of Barklem et al. (2000), on the fit of the H_α profile in the solar spectrum. Figure 12 shows this comparison, made with the same solar MARCS model, and the observed solar spectrum of Kurucz-Furenlid (2005). The differences between the two theoretical profiles obtained with the data of this paper and the Barklem data are very small, but neither give a very good fit with the observations, especially below 6570 Å. However, the theoretical profiles are very model dependent, as shown in a similar comparison made with the solar model of Holweger & Müller (1974) in Fig. 13.

4. Conclusion

In this paper we have focused on the self-broadening of the hydrogen Balmer α line and the variation of its line parameters with

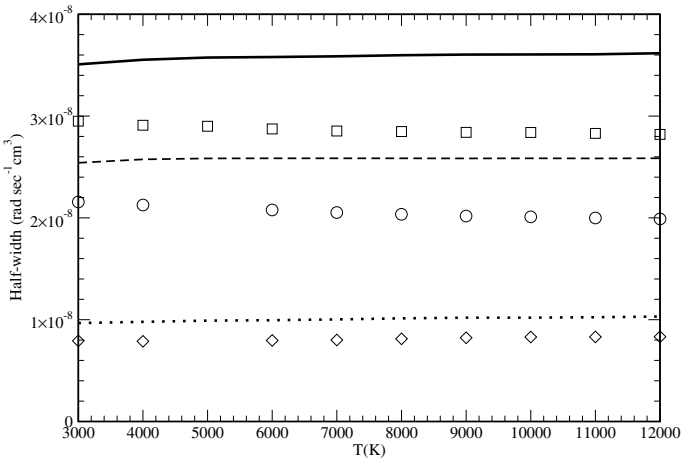

Fig. 9. Comparison of the line width of the contributions of the singlets and triplets to the 3d–2p component of H α. (—) 3d–2p averaged over velocity; (□) 3d–2p, using $\bar{v}$; (– – –) 3d–2p triplets only, averaged over velocity; (○) 3d–2p triplets only using $\bar{v}$; (· · ·) 3d–2p singlets only, averaged over velocity; (◇) 3d–2p singlets only, using $\bar{v}$.

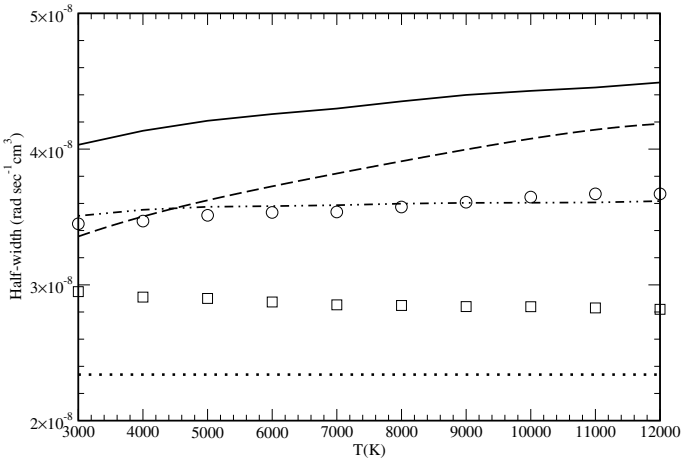

Fig. 10. Comparison of the line width due to H-H collisions with temperature in the different approaches. (—) Total of all contributions averaged over velocity; (– – –) Barklem et al. (2000b); (· · ·) Ali & Griem (1966); (○) total using $\bar{v}$; (– · · – · · –) 3d–2p only, averaged over velocity; (□) 3d–2p only, using $\bar{v}$.

Table 3. Comparison of the self-resonance broadening coefficients in rad s^{-1} cm^{-3} per perturber in the present paper and in Barklem et al. (2000b) Fig. 3.

T(K)	This paper	Barklem et al.
5000	0.421×10^{-7}	0.394×10^{-7}
6000	0.426×10^{-7}	0.402×10^{-7}
7000	0.430×10^{-7}	0.411×10^{-7}
8000	0.435×10^{-7}	0.419×10^{-7}
9000	0.440×10^{-7}	0.427×10^{-7}
10 000	0.443×10^{-7}	0.436×10^{-7}

temperature using complete potentials for the interactions of the atoms which have the correct asymptotic behavior and accurately represent the close collisions that are known to contribute to the line width. In our calculations, we took into account the 36 allowed transitions which contribute to the Balmer α line by using the energies and the transition moments of the molecular-electronic states of H_2 recently computed and

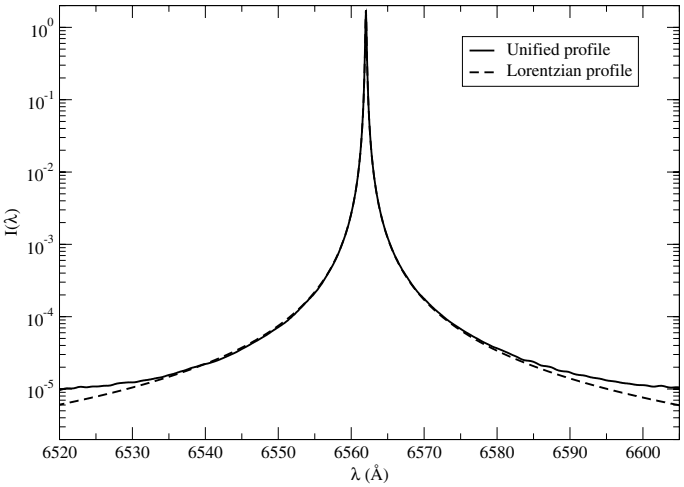

Fig. 11. Total unified line profile compared to the Lorentzian profile. (T = 4000 K, $n_{\rm H} = 1 \times 10^{18}$ cm^{-3}).

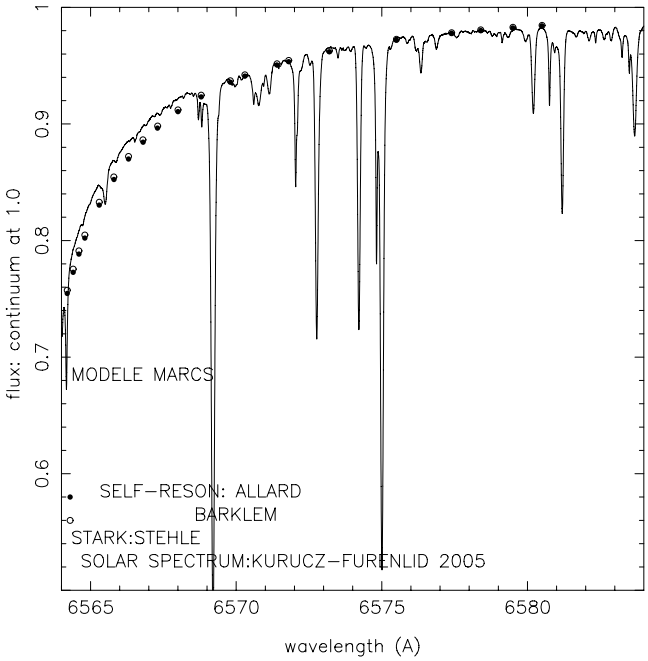

Fig. 12. Comparison of the theoretical profiles of H_α with the observed solar spectrum. Using the solar MARCS model.

Table 4. List of singlet and triplet transitions contributing to the 3d–2p component. The asymptotic transition moment d^2 is given in atomic units.

Singlet Transitions	Upper Level	Lower Level	d^2	Triplet Transitions	Upper Level	Lower Level	d^2
J–C	$1-{}^1\Delta_g$	$1-{}^1\Pi_u$	9	r–f	$2-{}^3\Pi_g$	$3-{}^3\Sigma_u^+$	4.5
D–GK	$2-{}^1\Pi_u$	$3-{}^1\Sigma_g^+$	4.5	du–i	$1-{}^3\Delta_u$	$1-{}^3\Pi_g$	4.5
W–I	$1-{}^1\Delta_u$	$1-{}^1\Pi_g$	9	k–a	$3-{}^3\Pi_u$	$1-{}^3\Sigma_g^+$	4.5
R′–B	$3-{}^1\Pi_g$	$1-{}^1\Sigma_u^+$	4.5	j–c	$1-{}^3\Delta_g$	$1-{}^3\Pi_u$	9
B4–GK	$4-{}^1\Sigma_u^+$	$3-{}^1\Sigma_g^+$	6	p–f	$4-{}^3\Sigma_g^+$	$3-{}^3\Sigma_u^+$	6
P–B	$5-{}^1\Sigma_g^+$	$1-{}^1\Sigma_u^+$	6	b5–a	$5-{}^3\Sigma_u^+$	$1-{}^3\Sigma_g^+$	6
R′–C	$3-{}^1\Pi_g$	$1-{}^1\Pi_u$	4.5	k–i	$3-{}^3\Pi_u$	$1-{}^3\Pi_g$	4.5
P–C	$5-{}^1\Sigma_g^+$	$1-{}^1\Pi_u$	1.5	b5–i	$5-{}^3\Sigma_u^+$	$1-{}^3\Pi_g$	1.5
D–I	$2-{}^1\Pi_u$	$1-{}^1\Pi_g$	4.5	p–c	$4-{}^3\Sigma_g^+$	$1-{}^3\Pi_u$	1.5
B4–I	$4-{}^1\Sigma_u^+$	$1-{}^1\Pi_g$	1.5	r–c	$2-{}^3\Pi_g$	$1-{}^3\Pi_u$	4.5

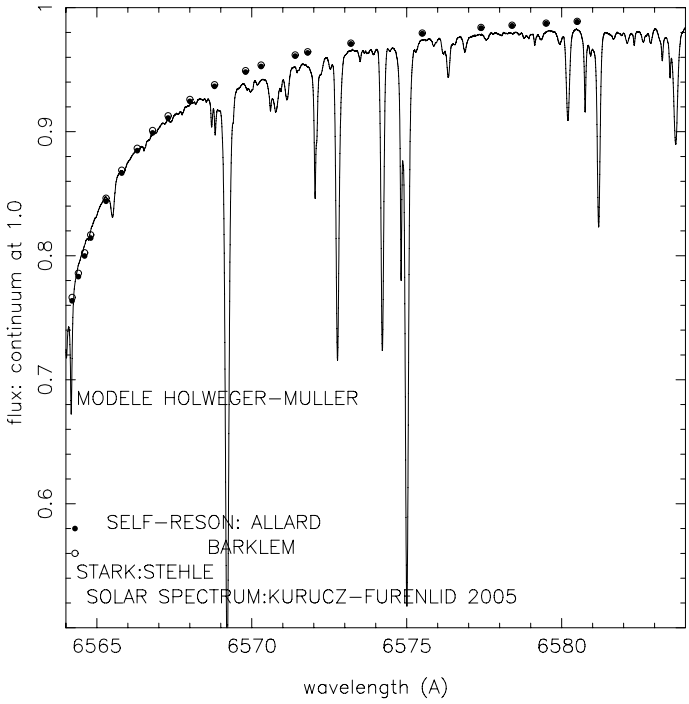

Fig. 13. Comparison of the theoretical profiles of H_α with the observed solar spectrum. Using the Holweger-Müller model.

carefully validated by Spielfiedel et al. (2004). Collision effects were computed in the framework of the impact limit of a unified theory of spectral line broadening of Allard et al. (1999). A total line profile outside the impact region was also computed with the same input data, and a comparison established a region of validity of the commonly used Lorentzian profile. It is shown that our calculations lead to significantly larger widths than the Ali & Griem theory (1966), and are closer to the recent work of Barklem et al. (2000a,b). The temperature dependence of the width of Balmer α when the complete potentials are taken into account, is less than Barklem et al. (2000a,b) found, and for solar type stars the width of Balmer α is about 5% larger than their result. Therefore, our independent analysis supports the conclusion of Barklem et al. (2000a,b) that useful models of the effect of neutral collisions in the Balmer series line cores must include details of the interactions beyond the long range resonance effects. We add here that including the full set of contributing components, having accurate intermediate to short range interactions, and averaging over velocity rather than using an average velocity are additional significant factors in the Balmer profile. It also appears that non-Lorentzian sources of opacity in the far wing are present. This may be useful for stellar diagnostics since the far wing arises from deeper layers in the stellar atmosphere where the neutral atom density is higher, and where convective processes are important in the stellar models.

This work provides a firm basis to the determination of effective temperatures of stars from the wings of Balmer lines. This criterion is now widely used because it has the advantage of being independent of the interstellar reddening which is not the case for photometric temperatures. A second paper shall develop this application.

References

Ali, A. W., & Griem, H. R. 1966, Phys. Rev. A, 144, 366
Allard, N. F., & Kielkopf, J. F. 1982, Rev. Mod. Phys., 54, 1103
Allard, N. F., & Biraud, Y. G. 1983, J. Phys., 44, 935
Allard, N. F., Koester, D., Feautrier, N., & Spielfiedel, A. 1994, A&AS, 108, 417
Allard, N. F., Royer, A., Kielkopf, J. F., & Feautrier, N. 1999, Phys. Rev. A, 60, 1021
Allard, N. F., Kielkopf, J. F., & Loeillet, B. 2004, A&A, 424, 347
Baranger, M. 1958a, Phys. Rev., 111, 481
Baranger, M. 1958b, Phys. Rev., 111, 494
Barklem, P. S., Piskunov, N., & O'Mara, B. J. 2000a, A&A, 355, L5
Barklem, P. S., Piskunov, N., & O'Mara, B. J. 2000b, A&A, 363, 1091
Cox, A. N. 1999, Allen's Astrophysical Quantities (New York: Springer-Verlag), 393
Holweger, H., & Müller 1974, Sol. Phys., 39, 19
Kolb, A. C., & Griem, H. R. 1958, Phys. Rev., 111, 2, 514
Kurucz, R. L. 1979, ApJS, 40, 1
Kurucz, R. L. 1993, CD-ROM 13, SAO, http://cfaku5.cfa.harvard.edu/
Kurucz, R. L. 2005, http://kurucz.harvard.edu/sun/fluxatlas2005/
Lortet, M. C., & Roueff, E. 1969, A&A, 3, 462
Roueff, E., & Van Regemorter, H. 1969, A&A, 1, 69
Royer, A. 1974, Can. J. Phys., 52, 1816
Royer, A. 1980, Phys. Rev. A, 22, 1625
Sahal-Bréchot, S. 1969, A&A, 2, 501
Spielfiedel, A. 2003, J. Mol. Spectrosc., 217, 162
Spielfiedel, A., Palmieri, P., & Mitrushenkov, A. O. 2004, Molec. Phys., 102, N0. 21, 2249
Stehlé, C., & Hutcheon, R. 1999, A&AS, 140, 93
Weisskopf, V. 1933, Phys. Z, 34, 1